

# MoDA: Multi-modal Diffusion Architecture for Talking Head Generation

Xinyang Li<sup>1,2</sup>, Gen Li<sup>2</sup>, Zihui Lin<sup>1,3</sup>, Yichen Qian<sup>†1,3</sup>, Gongxin Yao<sup>2</sup>, Weinan Jia<sup>1</sup>, Aowen Wang<sup>1,2</sup>, Weihua Chen<sup>1,3</sup>, Fan Wang<sup>1,3</sup>

<sup>1</sup>Xunguang Team, DAMO Academy, Alibaba Group, <sup>2</sup>Zhejiang University, <sup>3</sup>Hupan Lab

† Corresponding author.

[yichen.qyc@alibaba-inc.com](mailto:yichen.qyc@alibaba-inc.com), [1\\_xyang@zju.edu.cn](mailto:1_xyang@zju.edu.cn)

Talking head generation with arbitrary identities and speech audio remains a crucial problem in the realm of the virtual metaverse. Despite progress, current methods still struggle to synthesize diverse facial expressions and natural head movements while generating synchronized lip movements with the audio. The main challenge is stylistic discrepancies between speech audio, individual identity, and portrait dynamics. To address the challenge of inter-modal inconsistency, we introduce MoDA, a multi-modal diffusion architecture with two well-designed technologies. First, MoDA explicitly models the interaction among motion, audio, and auxiliary conditions, enhancing overall facial expressions and head dynamics. In addition, a coarse-to-fine fusion strategy is employed to progressively integrate different conditions, ensuring effective feature fusion. Experimental results demonstrate that MoDA improves video diversity, realism, and efficiency, making it suitable for real-world applications. Project Page: <https://lixinyyang.github.io/MoDA.github.io/>

**Date:** August 11, 2025



## 1 Introduction

Talking head generation aims to create a photorealistic, speaking portrait from a single image, guided by audio and other modalities. Combined with the generative adversarial network (GAN) [9] and diffusion model [28], recent methods demonstrate widespread potential applications, such as immersive telepresence, virtual characters, and augmented reality.

Diffusion models have recently marked a significant advancement in generative modeling, enabling the creation of highly diverse videos. Early diffusion-based methods [5, 33, 13, 38] generate the final video directly from the audio input. Although trainable from end to end, methods like Hallo2 [5] remain two major limitations persist, as shown in Fig. 2: 1) Inefficient inference process and visual artifacts. 2) Unnatural facial expressions and head movements with precise lip-sync. Recently, two-stage methods [39, 2, 15] have simplified the diffusion process by bypassing complex variational auto-encoder (VAE) decoding. Methods like VASA-1 [39] first use the diffusion model to generate intermediate motion representations from audio, and then use a separate rendering network to synthesize the final video. However, the final video quality is heavily dependent on the accuracy of these

intermediate representations. Thus, these methods still struggle to achieve natural facial dynamics with precise lip-sync due to suboptimal predictions.

Looking into the aforementioned issues, we argue that their root cause is the stylistic discrepancies between speech audio, individual identity, and portrait dynamics. These methods typically concatenate multiple conditions to form a mixed representation, which is then fed into a cross-attention mechanism where information flows only from this mixed modality to motion. This design introduces a learning bias, causing the model to focus only on the most shallow feature cues while neglecting the intricate relationships between the modalities. Consequently, it fails to handle more complex or conflicting scenarios. As in the ablation study, this limitation leads directly to inconsistent motion sequences when the model is conditioned on arbitrary identity input.

To address the challenge of inter-modal inconsistency, we propose MoDA, a novel framework designed for synergistic talking head generation. MoDA begins by operating within a joint parameter space that bridges motion generation and neural rendering, encompassing a disentangled motion-appearance space [11] along with audio, emotion, and identity. This space has a dimensionality that is an order of

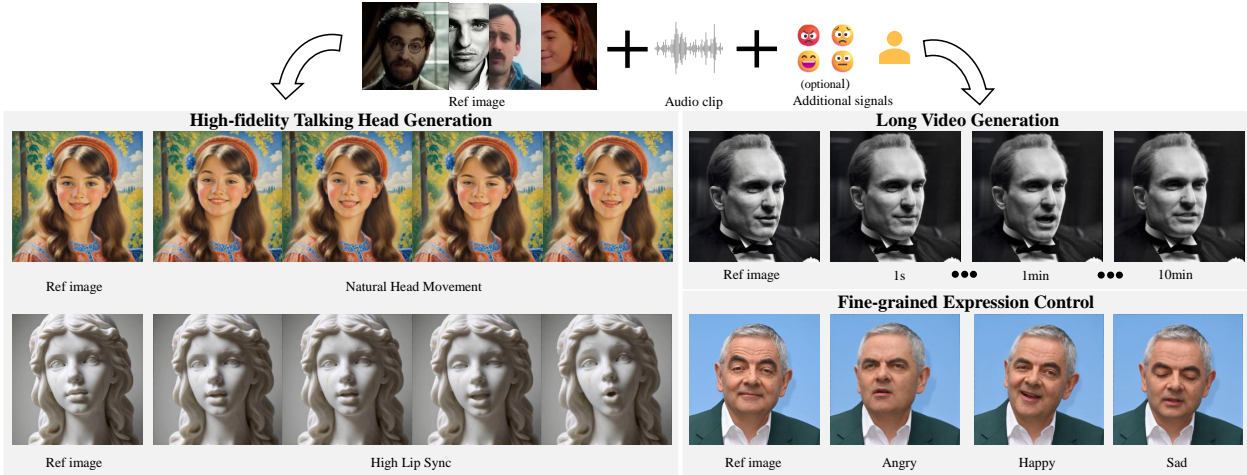


**Figure 1** Given a reference image, an audio clip, and other control signals, MoDA excels in producing vivid portrait animation videos in real-time. Beyond basic lip synchronization, it demonstrates strong capabilities in generating diverse facial expressions and natural head movements. Furthermore, it supports fine-grained facial expression control and long-term video synthesis.

magnitude lower than traditional VAE spaces, which dramatically reduces the complexity of multi-modal fusion. Moreover, by incorporating optional conditions like identity and emotion, MoDA makes the generative modeling of complex distribution more tractable and increases fine-grained control over the generative process.

MoDA is guided by two core principles designed to address these inconsistencies: 1) We draw inspiration from recent lip-to-speech tasks [35, 21], where visual information can provide additional context to complement the audio. As shown in Fig. 3, MoDA introduces the Multi-modal Diffusion Transformer (MMDiT) [8], equipped with rectified flow [17], as the framework to facilitate multi-modal fusion. In this design, MoDA can dynamically adapt audio features based on motion, identity, and emotion, thereby improving the accuracy of motion generation. 2) To systematically integrate these modalities based on semantic information, MoDA implements a coarse-to-fine fusion strategy. Initially, the model uses separate weights to capture the unique characteristics of each modality. In the intermediate stage, a unified representational space is introduced for semantically linked modalities like audio, emotion, and identity to form a unified motion command. Finally, all modalities are integrated into a unified representation space, allowing holistic fusion. To further encourage precise lip-sync while maintaining motion diversity, MoDA provides an optional Adaptive Lip-motion sync Expert (ALSE), which can be integrated during training. The contributions can be summarized as follows:

- This paper proposes MoDA, a novel multi-modal

diffusion framework that generates high-fidelity talking head videos from an image, audio, and additional modalities.

- A coarse-to-fine fusion strategy is designed to progressively integrate noisy motion with audio and other modalities, enabling effective multi-modal fusion.
- Extensive evaluations on public datasets demonstrate that our method outperforms contemporary alternatives in visual quality and quantitative metrics.

## 2 Related Work

### 2.1 Disentangled Face Representation

In recent years, extensive research has been conducted on disentangled facial representation learning. Some methods utilize sparse keypoints [27, 44] or 3D Morphable Model (3DMM) [1, 16] techniques to explicitly represent facial dynamics. The 3DMM initially projects the 3D head shape into several low-dimensional Principal Component Analysis (PCA) spaces, which provide orthogonal bases. Based on these orthogonal bases, attributes such as identity, pose, and expression can be manipulated in the 3D model using linear blend skinning (LBS). However, these methods may face issues such as inaccurate reconstructions or limited ability to decouple facial attributes. Recent learning-based approaches, such as Face Vid2Vid [37], LivePortrait [11], and Megaportrait [7], have been introduced to disentangle facial representations within a nonlinear parameter space,

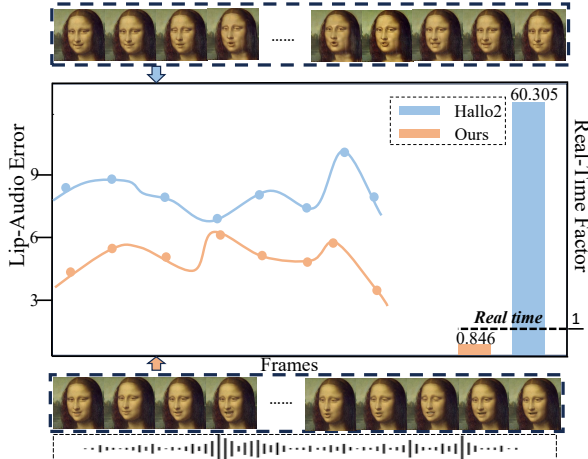


**Figure 2** Comparison of our approach with hallo2 [5]. Real-Time Factor (RTF) measures the ratio of inference time to output duration. An RTF  $< 1$  indicates that the system can perform real-time generation. Frame-by-frame comparison. Hallo2 shows lower lip synchronization, inference efficiency, and identity consistency than our method.

significantly enhancing the expressive power of these models. Moreover, by leveraging a more compact parameterization, these methods can effectively capture intricate details and dynamic facial expressions, offering greater flexibility in both facial reconstruction and animation.

## 2.2 Audio-driven Talking Head Generation

In audio-driven digital human technology, one-shot methods have gained considerable attention, enabling the generation of dynamic and expressive avatars from a single image input. Existing methods can generally be classified into two categories: single-stage and two-stage audio-to-video generation. The former [13, 5, 22, 26, 38, 10, 6] directly maps audio features to video frames in an end-to-end manner. In contrast, the latter [15, 39, 2, 30, 45] introduces an intermediate representation, such as motion sequences or keypoints, serving as a bridge between audio and video synthesis.

Early single-stage methods [10, 22, 31] leveraged GANs to focus on lip-sync accuracy while keeping other facial attributes unchanged. Recent advancements have incorporated diffusion-based approaches [38, 26, 5, 33, 3], expanding the scope of research by mapping audio inputs to diverse facial expressions and continuous natural head movements. However, these methods rely on denoising and rendering images within the VAE space, where appearance and motion remain highly entangled, resulting in substantial computational overhead and low inference

efficiency.

The two-stage methods address the above limitations by introducing a disentangled facial space as an intermediate representation. Early methods [41, 42] used explicit landmarks or 3DMM as intermediate representations to bridge the gap between audio inputs and animated outputs, allowing for more controllable and interpretable motion synthesis. Recently, VASA-1 [39], Ditto [15], and JoyVASA [2] have shifted towards implicit facial representations [37, 7, 11] while employing DIT-based models for audio-to-motion mapping, leading to more expressive and natural video synthesis. However, relying solely on cross-attention for lip-sync generation neglects the rich multimodal interactions and deep-level information within the input signals, thereby limiting the diversity and expressiveness of the generated outputs.

## 3 Method

### 3.1 Preliminaries

Denoising Diffusion probabilistic models (DDPMs) [29] have emerged as a powerful framework for generative modeling by formulating the data generation process as an iterative denoising procedure. In the forward diffusion process, Gaussian noise  $\epsilon$  is gradually introduced into the data distribution across  $T$  discrete timesteps, producing noisy latent features:  $z_t = \sqrt{\alpha_t}z_0 + \sqrt{1 - \alpha_t}\epsilon$ , where  $\alpha_t$  represents a variance schedule that determines the noise level at each timestep, and  $z_0$  is the raw data. The model is trained to reverse this process by taking the noisy latent representation  $z_t$  as input and estimating the added noise  $\epsilon$ . The training objective is defined as:  $\mathcal{L} = \mathbb{E}_{z_t, c, \epsilon \sim \mathcal{N}(0, 1), t} [\|\epsilon - \epsilon_\theta(z_t, t, c)\|_2^2]$ , where  $\epsilon_\theta$  denotes the noise prediction generated by the model, and  $c$  represents additional conditioning signals, such as audio or motion frames, which are particularly relevant in the generation of talking videos.

Recently, Stable Diffusion 3 (SD3) [8] has advanced the paradigm by introducing Rectified Flow [20, 17] that optimizes the traditional DDPMs objective:

$$\mathcal{L} = \mathbb{E}_{z_t, c, \epsilon \sim \mathcal{N}(0, 1), t} [\|(\epsilon - z_0) - v_\theta(z_t, t, c)\|_2^2], \quad (1)$$

where  $z_t = (1 - t)z_0 + t\epsilon$ , and  $v_\theta$  denotes the velocity field. After the rectified flow training is completed, the transition from  $\epsilon$  to  $z_0$  can be formulated using the numerical integration of an ordinary differential equation (ODE):

$$z_{t - \frac{1}{N}} = z_t + \frac{1}{N}v_\theta(z_t, t, c), \quad (2)$$

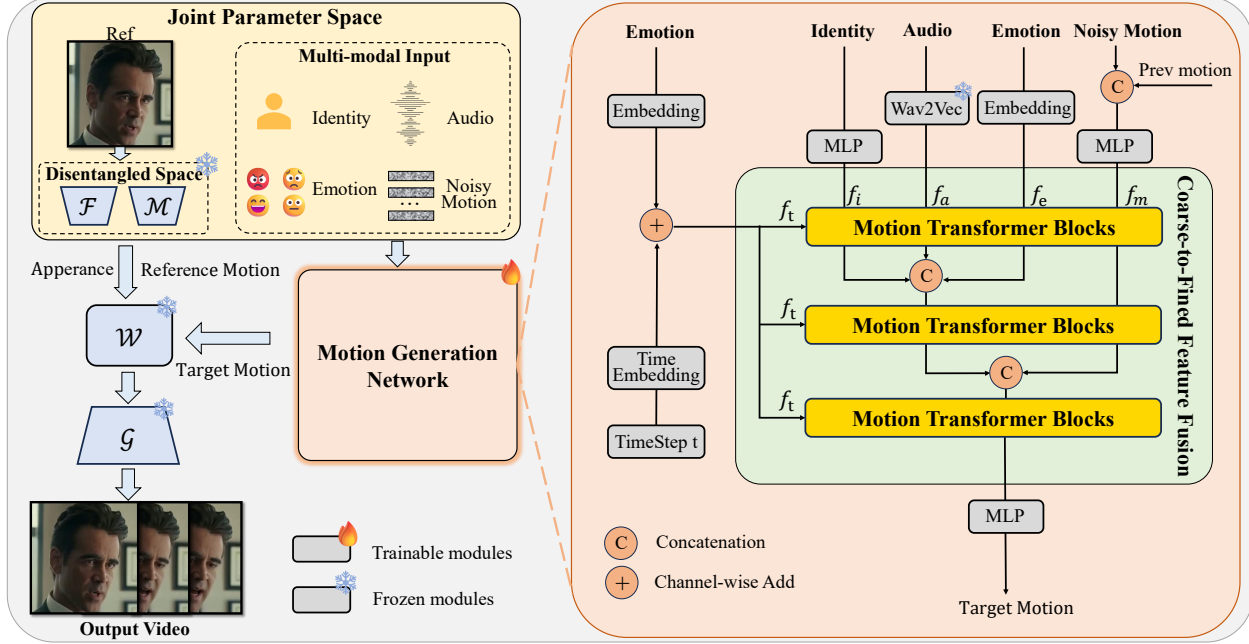


**Figure 3** Overall architecture of the proposed MoDA and illustration of our Motion Generation Network. The appearance extractor  $\mathcal{F}$ , motion extractor  $\mathcal{M}$ , warping module  $\mathcal{W}$ , and decoder  $\mathcal{G}$  are frozen. A motion feature generation model based on a Diffusion Transformer is then trained to generate motion features.

where  $N$  denotes the discretization steps of the interval  $[0, 1]$ . The piecewise linear denoising process improves training stability. Furthermore, since our audio-to-motion task does not involve complex pixel information, this approach is particularly well-suited to our needs. Given these advantages, we adopt the rectified flow for training.

## 3.2 Model Architecture

Instead of simply concatenating these conditioning signals, we enhance the intrinsic characteristics and emotional nuances of the audio representation by treating external emotion and identity cues as "catalysts". This approach balances identity and emotion between audio and speakers, enabling more natural lip control in real-world scenarios.

### 3.2.1 Joint Parameter Space

As shown in Fig. 3, we incorporate the existing facial re-enactment framework [11] to extract disentangled facial representations. Specifically, the motion extractor  $\mathcal{M}$  yields expression deformations  $\delta$ , head pose parameters  $(R, t)$ , the canonical keypoints of the source image  $x_c$ , and a scaling factor  $S$ . The motion representation  $(R_s, \delta_s, t_s, S_s) \in \mathbb{R}^{70}$ , serves as an identity-agnostic representation of the source input and is used to train MoDA to predict  $(\hat{R}, \hat{\delta}, \hat{t}, \hat{S})$

given audio input.

$$x_s = S_s \cdot (x_c R_s + \delta_s) + t_s \quad , \quad \hat{x} = \hat{S} \cdot (x_c \hat{R} + \hat{\delta}) + \hat{t} \quad . \quad (3)$$

Subsequently, the warping field estimator  $\mathcal{W}$  computes a field from  $x_s$  and  $\hat{x}$  to deform the 3D features  $f_s$ , which are then passed to the generator  $\mathcal{G}$  to synthesize the target image. The audio features  $f_a$  are extracted using the wav2vec [24] encoder. To maintain consistency in the identity feature space across various scenarios, we use the canonical keypoints of the source image  $x_c$  as identity information and generate identity features  $f_i$ . For facial emotion signals, we use a visual emotion classifier [23] to extract the speaker's emotional labels and encode them into corresponding features  $f_e$ . The motion features from the first frame of each clip are used as guiding conditions to ensure inter-frame continuity and generate noisy motion features  $f_m$ . Inspired by EMO2 [32], emotion features  $f_e$  are added to timestep embeddings to generate timestep features  $f_t$ , which are injected into each motion transformer block by adaptive layer normalization (AdaLN) [19]. AdaLN is used to prevent the degradation of emotion features during the joint-attention operation, ensuring that emotional cues are preserved throughout the fusion. By integrating these conditioning signals, our model effectively generates realistic and temporally consistent motion features.

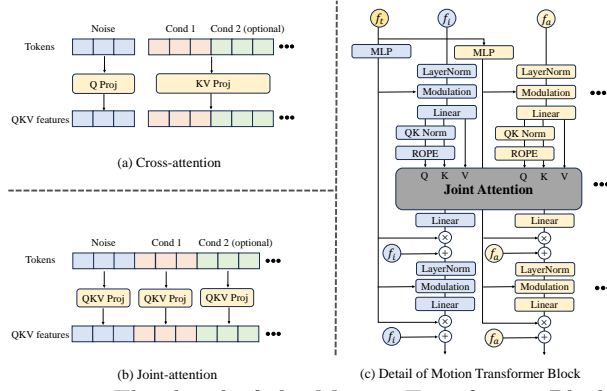


**Figure 4** The detail of the Motion Transformer Block and the Joint-attention. (a) Cross-attention uses noise as the query and conditions as key and value. (b) Joint-attention projects noise and conditions separately and concatenates them before attention.

### 3.2.2 Motion Transformer Blocks

As shown in Fig. 4 (c), the Motion Transformer Block consists of three main components: Modality-specific paths, Joint-attention and Rotational Position Encoding.

Modality-specific paths are designed to distinguish representations from different modalities. Specifically, each modality is equipped with its own adaLN and a modulation mechanism [19] to improve the conditional generation capabilities of the model.

Joint-attention is employed to enable interaction across different modalities. All modalities are first projected onto their respective query (Q), key (K), and value (V) representations, which are then concatenated in order along the sequence dimension. The combined sequence is processed through an attention operation, after which the attended features are split back into their respective modalities in the original order.

To enhance temporal alignment between noisy motion and other conditional features, we adopt Rotational Positional Encoding (RoPE) [40] instead of the absolute positional encoding used in MMDiT. Specifically, we first expand the expression and identity features to match the sequence length of the noisy motion and audio features. We then apply aligned RoPE across all modalities, which facilitates better temporal synchronization and more consistent feature representations.

### 3.2.3 Coarse-to-Fined Feature Fusion

Although assigning modality-specific paths with separate QKV projections and FeedForward Networks

(FFNs) in the attention mechanism can enhance multi-modal information, this design often overlooks the inherent semantic commonalities shared across modalities. Independently learned weights hinder effective multi-modal feature fusion and introduce redundant parameters, potentially causing inconsistency issues. This issue is particularly pronounced in tasks like audio-to-motion generation, where no pixel-level inputs are involved, and the semantic gap between modalities is relatively small. In such cases, maintaining entirely separate parameterizations fails to provide meaningful benefits and instead leads to duplicated representations. To enhance the model’s capacity for multi-modal understanding, we introduce a Coarse-to-Fine Feature Fusion strategy. This fusion strategy progressively integrates multi-modal features while reducing unnecessary parameters, thereby enhancing the multi-modal understanding and training stability.

As illustrated in Fig. 3, the architecture progresses through three stages: a four-stream, two-stream, and single-stream process. In the four-stream stage, each modality is processed independently to learn modality-specific representations, facilitating early-stage feature differentiation. In the two-stream stage, the audio stream is concatenated with emotion and identity features to form a merged stream that shares weights. This design encourages a balanced integration of emotional and identity cues from both the audio and the reference image. Finally, all modalities are unified into a single representation stream to allow deeper fusion and enhance generative expressiveness.

### 3.2.4 Loss Function

Our loss function utilizes the rectified flow loss and Eq. refeq:2 is rewritten as:

$$\mathcal{L}_{RF} = \mathbb{E}_{z_t, c, \epsilon \sim \mathcal{N}(0, 1), t} [ \|x - v_\theta(z_t, t, c)\|_2^2 ], \quad (4)$$

where  $x$  represents  $\epsilon - z_0$ ,  $v_\theta$  denotes the velocity field. The velocity loss  $\mathcal{L}_{vel}$  is introduced to encourage improved temporal consistency:

$$\mathcal{L}_{vel} = \|x' - m'\|_2^2 + \|x'' - m''\|_2^2, \quad (5)$$

where  $m$  denotes the output of  $v_\theta(z_t, t, c)$ , and  $m'$ ,  $m''$  denote the first-order and second-order derivatives of  $m$ . To further enforce lip-sync accuracy, we design the ALSE pretrained in audio and motion features and compute the loss  $\mathcal{L}_{ALSE}$ . It is worth noting that supervision from the pretrained ALSE is optional and can be applied as needed. In summary,

**Table 1** Comparison with existing methods on the HDTF and CelebV-HQ test sets.  $\uparrow$  Higher is better.  $\downarrow$  Lower is better. Best results are in **bold**, second-best are underlined.

Dataset	Method	FVD $\downarrow$	FID $\downarrow$	F-SIM $\uparrow$	Sync-C $\uparrow$	Sync-D $\downarrow$	Smo(%) $\uparrow$
HDTF	GT	-	-	0.860	7.267	7.586	0.9959
	EchoMimic	207.987	<u>29.633</u>	0.887	2.744	11.805	0.9939
	JoyHallo	256.226	44.842	0.852	7.360	7.984	0.9944
	Hallo	216.573	34.350	0.878	7.087	7.941	0.9950
	Hallo2	229.806	34.426	0.871	7.102	7.976	0.9951
	Ditto	243.491	32.200	<u>0.943</u>	6.102	8.790	0.9970
	JoyVASA	229.634	32.584	<b>0.953</b>	5.255	9.600	0.9968
	<b>Ours (sync)</b>	<u>191.292</u>	30.449	0.925	<b>8.183</b>	<b>7.065</b>	<u>0.9970</u>
	<b>Ours</b>	<b>174.622</b>	<b>28.182</b>	0.927	<u>7.369</u>	<u>7.744</u>	<b>0.9971</b>
CelebV-HQ	GT	-	-	0.861	5.837	7.989	0.9964
	EchoMimic	258.451	47.169	0.837	2.610	11.216	0.9946
	JoyHallo	282.081	<u>57.247</u>	0.813	<u>6.041</u>	8.418	0.9945
	Hallo	245.101	44.411	0.851	5.629	8.384	0.9952
	Hallo2	242.352	46.615	0.851	5.671	8.397	0.9953
	Ditto	302.525	46.996	0.915	4.681	9.280	<b>0.9973</b>
	JoyVASA	271.231	44.574	<b>0.918</b>	5.171	8.632	0.9971
	<b>Ours (sync)</b>	<b>205.307</b>	<u>44.201</u>	<u>0.916</u>	<b>6.552</b>	<b>7.635</b>	<u>0.9972</u>
	<b>Ours</b>	<u>205.442</u>	<b>44.071</b>	0.913	5.878	<u>8.135</u>	0.9972

the final loss can be expressed as follows:

$$\mathcal{L} = \mathcal{L}_{RF} + \mathcal{L}_{vel} + \lambda_{sync} \cdot \mathcal{L}_{ALSE} \quad , \quad (6)$$

$$\lambda_{sync} = \begin{cases} 1, & \text{if } \mathcal{L}_{ALSE} < \tau \\ 0, & \text{otherwise} \end{cases} \quad , \quad (7)$$

where  $\tau$  is set to 0.4 and controls when the synchronization loss is activated, ensuring that lip-motion supervision is applied only after basic motion diversity has been established. Further details about the Adaptive Lip-motion Synchronization Expert (ALSE) can be found in the supplementary materials.

### 3.3 Realtime Inference

The real-time conversational scenario is enabled by low-latency motion generation. We align audio features with the video frame rate and segment the audio into continuous 100-frame chunks for streaming generation. Additionally, leveraging low-dimensional intermediate representations and the rectified flow, we reduce DiT inference denoising steps from 50 to 10, yet achieve even higher quality. For detailed comparison, please refer to the supplementary material.

#### 3.3.1 Classifier-free guidance (CFG)

In the training stage, we randomly assign each of the input conditions, and during inference, we perform the following:

$$\hat{z}^0 = (1 + \sum_{c \in C} \lambda_c) \cdot v_\theta(z^t, t, C) - \sum_{c \in C} \lambda_c \cdot v_\theta(z^t, t, C|c = \emptyset), \quad (8)$$

where  $\lambda_c$  is the CFG scale of condition  $c$ .  $C|c = \emptyset$  denotes that the condition  $c$  is  $\emptyset$ .

## 4 Experiments

### 4.1 Experiment Settings

#### 4.1.1 Dataset and Metrics

MoDA is primarily trained on three publicly available datasets: HDTF [46], CelebV-Text [43], and MEAD [36]. For evaluation, we conducted experiments on three distinct test sets. The first two are derived from public datasets, CelebV-HQ [47] and HDTF, each consisting of 50 randomly sampled clips ranging from 3 to 10 seconds in length. The third is an in-the-wild set with 20 diverse cases, including real individuals, animated characters, dynamic scenes, and complex headwear. Each sample is paired with audio that is speech, emotional dialogue, or singing. We utilize several evaluation metrics to assess the performance of the proposed method. The Fréchet Inception Distance (FID) [25] and the Fréchet Video Distance (FVD) [34] are used to assess the quality of the generated output, while the F-SIM [33] measures facial similarity. In addition, Sync-C [4] and Sync-D [4] metrics are introduced to evaluate lip-synchronization between different methods. A temporal smoothness metric (Smo) [12] is also utilized to monitor the continuity of generated motion.

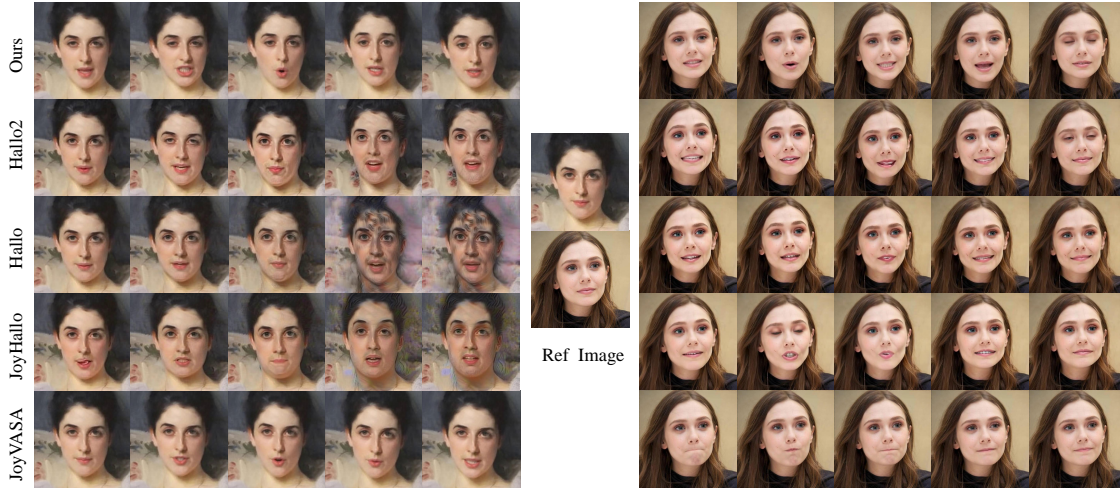


**Figure 5** Qualitative Comparisons with State-of-the-Art Method. As single-frame images cannot fully represent synchronization, naturalness, and stability, we provide complete video comparisons in the supplementary materials.

#### 4.1.2 Implementation Details

During training, we randomly sample 80-frame segments from video clips to train the motion generation model. The model is trained for approximately 500 epochs on 8 NVIDIA H20 GPUs with a batch size of 512, using the Adam optimizer with a learning rate of 1e-4. During training, we apply a dropout probability of 0.1 for each emotion condition, while the dropout probability for speech is set to 0.5. Furthermore, the model is structured with 3 four-stream blocks, 6 two-stream blocks, and 12 single-stream blocks to progressively enhance multi-modal feature integration.

**Table 2** Comparison with existing methods on the wild test dataset. The best results are bold, and the second are underlined.

Method	F-SIM $\uparrow$	Sync-C $\uparrow$	Sync-D $\downarrow$	RTF $\downarrow$
EchoMimic	0.870	2.292	12.130	48.657
JoyHallo	0.825	<u>7.000</u>	8.167	59.735
Hallo	0.848	6.051	8.730	59.190
Hallo2	0.849	6.386	8.523	60.305
Ditto	<u>0.923</u>	6.107	9.040	<b>0.792</b>
JoyVASA	<b>0.924</b>	5.569	9.368	1.717
<b>Ours (sync)</b>	0.896	<b>7.710</b>	<b>7.469</b>	<u>0.846</u>
<b>Ours</b>	0.895	6.862	<u>8.088</u>	<u>0.846</u>

## 4.2 Results and Analysis

We juxtapose the results of the proposed method against those of EchoMimic [3], Ditto [15], JoyVASA [2], JoyHallo [26], Hallo [38], and Hallo2 [5], Ours and Ours (Sync) (MoDA with ALSE).

#### 4.2.1 Quantitative Comparison

The quantitative results on the CelebV-HQ test and HDTF dataset are shown in Table 1. On the HDTF dataset, MoDA consistently outperforms all existing methods across all evaluation metrics. In particular, our method achieves the lowest FID and FVD scores, outperforming the second-best methods by 4.9 % and 16.0 %, respectively. This demonstrates the superiority of our method in terms of visual naturalness and the overall quality of the generated frames. The two-stage methods better preserve identity, as evidenced by their F-SIM scores. Notably, JoyVASA and Ditto achieve the highest and second-highest F-SIM, respectively—likely due to their relatively constrained head movements and facial expressions, which enhance frame-wise structural similarity. The correspondingly lower FVD scores further reflect these limitations. In contrast, MoDA effectively mitigates such issues, demonstrating that enhancing multi-modal fusion can lead to improved overall model performance.

On the CelebV-HQ test dataset, MoDA consistently outperforms the six baseline methods in all metrics except Sync-D and Smo, highlighting its robustness. Although MoDA slightly underperforms JoyHallo in synchronization confidence (Sync-C), it achieves a notable improvement in synchronization distance (Sync-D), along with further gains in motion smoothness. Tables 1 also reports the results with and without ALSE. Introducing ALSE to supervise the synchronization between audio and keypoints leads to a significant improvement in lip-sync.

Table 2 shows that our method outperforms existing approaches across multiple metrics on the wild test set with diverse identities. We also report the real-

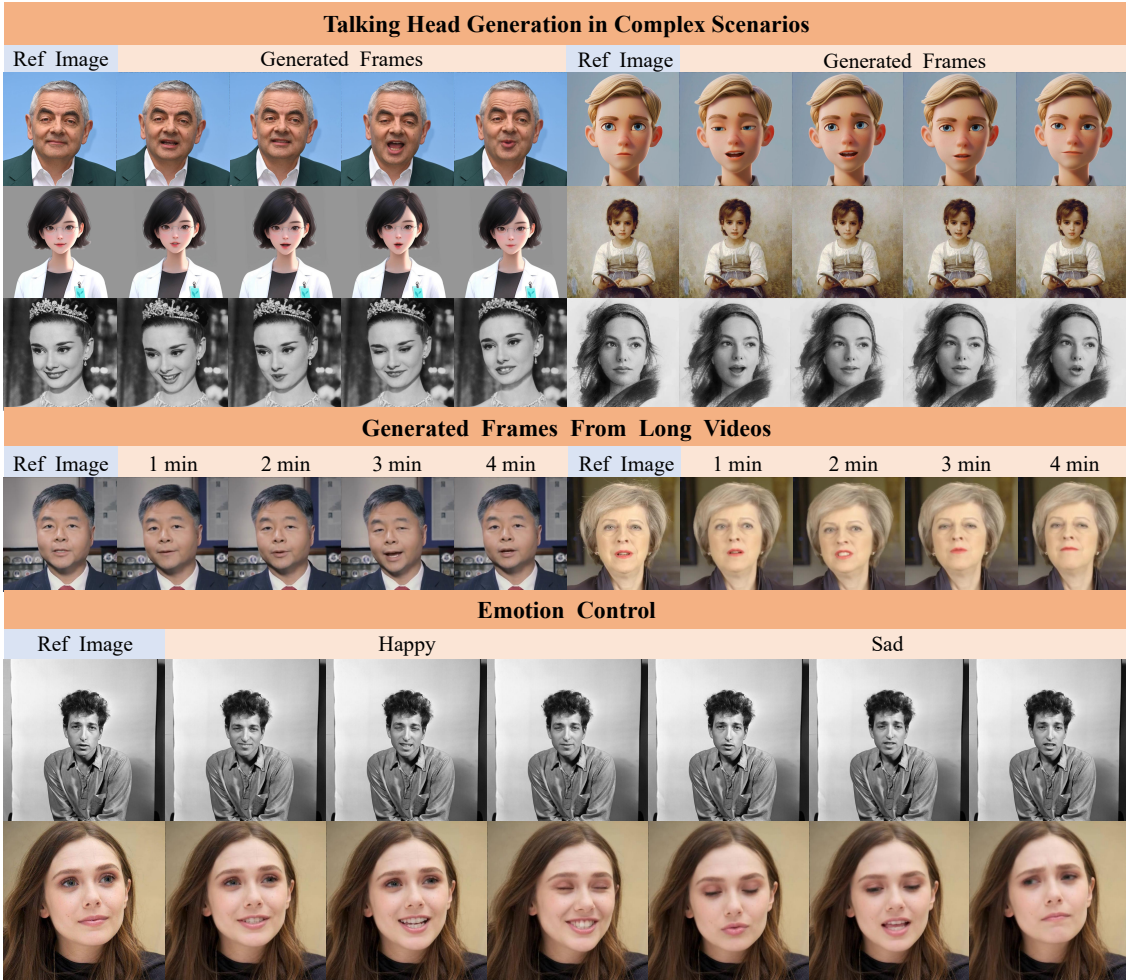


**Figure 6** Generation results for portraits and audio in diverse styles are presented. We also demonstrate long-video inference and fine-grained control over facial expressions.

time factor (RTF), where  $RTF < 1$  indicates real-time capability. Ditto achieves the lowest RTF, benefiting from TensorRT acceleration. Our method also delivers competitive efficiency, demonstrating its suitability for real-world applications.

#### 4.2.2 Qualitative Evaluation

As shown in Fig. 5, we selected two types of cases from the wild dataset for visual comparison. For each character, we generated videos using each method and selected frames from the same location for comparison. Analyzing the results, previous one-stage-based methods, including Hallo2, Hallo, and JoyHallo, suffer from appearance blurring and unnatural expressions during temporal inference due to the strong entanglement between appearance and motion. In contrast, our proposed two-stage framework effectively mitigates these issues, ensuring high consistency in the generated details. Compared to the two-stage method JoyVASA, MoDA generates richer expres-

sions, better lip-synchronization, and more natural head movements, thanks to our multi-modal motion generation network, which effectively integrates deep information across different modalities.

#### 4.2.3 Visualization Results in Complex Scenarios.

We further investigate MoDA’s generation performance in complex scenarios. Specifically, for the visual modality, we utilize portraits of both real humans and animated characters, each paired randomly with various audio types, including speech, singing, recitation, and others. As shown in Fig. 6, our method

**Table 3** Ablation study results on major architectural choices.

Method	FID $\downarrow$	FVD $\downarrow$	Sync-C $\uparrow$	Sync-D $\downarrow$
w/ CABA	47.365	232.291	5.331	8.692
w/o C2F	44.548	221.631	5.535	8.465
w/ MAF	48.358	216.982	5.511	8.527
Full Model	44.071	205.442	5.878	8.135

demonstrates strong performance in various complex scenarios. In addition, it is capable of efficient long-duration inference and fine-grained facial expression control.

### 4.3 Ablation Study

For more ablation experiments and implementation details, please refer to the supplementary materials.

#### 4.3.1 Cross-attention

We replace the MoDA with a Cross-Attention-Based Architecture (CABA) to perform multi-modal fusion for evaluation purposes. As shown in Table 3, this substitution results in a performance drop in all metrics. Moreover, as illustrated in Fig. 7, the subject exhibits mouth-closing failures when lacking deep multi-modal interaction. To investigate this, we conducted two experiments under the same settings used in the w/ CABA variant as shown in Fig. 7: 1) replacing the audio with the same image did not resolve the mouth closure issue (Replace audio); 2) replacing the image with the same audio addressed the issue (Replace image). These results suggest that cross-attention fails to adapt audio features to different identity conditions. In contrast, MoDA enables dynamic adaptation of audio features based on contextual factors such as motion, identity, and emotion.

#### 4.3.2 Coarse-to-Fine Feature Fusion

We replace the Coarse-to-Fine Feature Fusion with a fully four-stream architecture (w/o C2F). As shown in Table 3, this design leads to performance degradation, particularly in synchronization and motion quality, emphasizing the necessity of progressive feature fusion for effective cross-modal integration. These results indicate that independent learning of weights introduces substantial redundant parameters, resulting in convergence challenges (with 904M parameters in the w/o C2F variant). In contrast, by gradually sharing weights, the proposed coarse-to-fine strategy significantly reduces the parameter count to 370M, leading to both greater efficiency and improved performance.

To further investigate the effectiveness of the fusion strategy, we modified the original dual-stream design by creating an MAF variant that first merges motion with the auxiliary cues (emotion + identity) into one branch, while audio stays in the other. Table 3 also shows that MAF performs worse than even the w/o C2F baseline. Directly fusing the heterogeneous noisy motion and auxiliary condition features confuses the network. Our full model first merges audio with



**Figure 7** Visualization of ablation studies on key components.

the auxiliary cues; speech audio inherently carries emotion and identity signals, providing a natural bridge and delivering better accuracy and efficiency.

### 4.4 Discussion

For the disentanglement stage, we can use alternatives such as MegaPortraits or Face Vid2Vid, but like LivePortrait they degrade on large pose changes or when the subject wears complex head accessories. This may be due to limitations in the training data or intrinsic constraints of the GAN-based architecture. To address these challenges, we plan to improve the training dataset by incorporating a wider range of variations in head poses and complex head accessories. Furthermore, we will investigate more advanced video generation models [14, 18] to improve the quality and expressiveness of the generated results.

## 5 Conclusion

We propose MoDA, a two-stage multi-modal diffusion framework for one-shot talking head generation. MoDA effectively leverages multi-modal information to map audio to motion sequences in an identity-agnostic latent space, which are then translated into video frames by a pre-trained face renderer. From a single portrait, MoDA produces high-quality, expressive, and controllable talking head videos, surpassing previous methods in quality, diversity, and naturalness with high efficiency.

## References

- [1] Volker Blanz and Thomas Vetter. A morphable model for the synthesis of 3d faces. In *Proceedings of the 26th annual conference on Computer graphics and interactive techniques - SIGGRAPH '99*, Jan 1999.
- [2] Xuyang Cao, Guoxin Wang, Sheng Shi, Jun Zhao, Yang Yao, Jintao Fei, and Minyu Gao. Joyvasa: Portrait and animal image animation with diffusion-based audio-driven facial dynamics and head motion generation. *arXiv preprint arXiv:2411.09209*, 2024.
- [3] Zhiyuan Chen, Jiajiong Cao, Zhiqian Chen, Yuming Li, and Chenguang Ma. Echomimic: Lifelike audio-driven portrait animations through editable landmark conditions. *arXiv preprint arXiv:2407.08136*, 2024.
- [4] Joon Son Chung and Andrew Zisserman. Out of time: automated lip sync in the wild. In *Computer Vision-ACCV 2016 Workshops: ACCV 2016 International Workshops, Taipei, Taiwan, November 20-24, 2016, Revised Selected Papers, Part II 13*, pages 251–263. Springer, 2017.
- [5] Jiahao Cui, Hui Li, Yao Yao, Hao Zhu, Hanlin Shang, Kaihui Cheng, Hang Zhou, Siyu Zhu, and Jingdong Wang. Hallo2: Long-duration and high-resolution audio-driven portrait image animation. *arXiv preprint arXiv:2410.07718*, 2024.
- [6] Jiahao Cui, Hui Li, Yun Zhan, Hanlin Shang, Kaihui Cheng, Yuqi Ma, Shan Mu, Hang Zhou, Jingdong Wang, and Siyu Zhu. Hallo3: Highly dynamic and realistic portrait image animation with diffusion transformer networks. *arXiv preprint arXiv:2412.00733*, 2024.
- [7] Nikita Drobyshev, Jenya Chelishev, Taras Khakhulin, Aleksei Ivakhnenko, Victor Lempitsky, and Egor Zakharov. Megaportraits: One-shot megapixel neural head avatars. In *Proceedings of the 30th ACM International Conference on Multimedia*, pages 2663–2671, 2022.
- [8] Patrick Esser, Sumith Kulal, Andreas Blattmann, Rahim Entezari, Jonas Müller, Harry Saini, Yam Levi, Dominik Lorenz, Axel Sauer, Frederic Boesel, et al. Scaling rectified flow transformers for high-resolution image synthesis. In *Forty-first international conference on machine learning*, 2024.
- [9] Ian J Goodfellow, Jean Pouget-Abadie, Mehdi Mirza, Bing Xu, David Warde-Farley, Sherjil Ozair, Aaron Courville, and Yoshua Bengio. Generative adversarial nets. *Advances in neural information processing systems*, 27, 2014.
- [10] Jiazhi Guan, Zhanwang Zhang, Hang Zhou, Tianshu Hu, Kaisiyuan Wang, Dongliang He, Haocheng Feng, Jingtuo Liu, Errui Ding, Ziwei Liu, et al. Stylesync: High-fidelity generalized and personalized lip sync in style-based generator. In *Proceedings of the IEEE/CVF Conference on Computer Vision and Pattern Recognition*, pages 1505–1515, 2023.
- [11] Jianzhu Guo, Dingyun Zhang, Xiaoqiang Liu, Zhizhou Zhong, Yuan Zhang, Pengfei Wan, and Di Zhang. Liveportrait: Efficient portrait animation with stitching and retargeting control. *arXiv preprint arXiv:2407.03168*, 2024.
- [12] Ziqi Huang, Yinan He, Jiashuo Yu, Fan Zhang, Chenyang Si, Yuming Jiang, Yuanhan Zhang, Tianxing Wu, Qingyang Jin, Nattapol Chanpaisit, et al. Vbench: Comprehensive benchmark suite for video generative models. In *Proceedings of the IEEE/CVF Conference on Computer Vision and Pattern Recognition*, pages 21807–21818, 2024.
- [13] Jianwen Jiang, Chao Liang, Jiaqi Yang, Gaojie Lin, Tianyun Zhong, and Yanbo Zheng. Loopy: Taming audio-driven portrait avatar with long-term motion dependency. In *The Thirteenth International Conference on Learning Representations*, 2024.
- [14] Weijie Kong, Qi Tian, Zijian Zhang, Rox Min, Zuozhuo Dai, Jin Zhou, Jiangfeng Xiong, Xin Li, Bo Wu, Jianwei Zhang, et al. Hunyuanyvideo: A systematic framework for large video generative models. *arXiv preprint arXiv:2412.03603*, 2024.
- [15] Tianqi Li, Ruobing Zheng, Minghui Yang, Jingdong Chen, and Ming Yang. Ditto: Motion-space diffusion for controllable realtime talking head synthesis. *arXiv preprint arXiv:2411.19509*, 2024.
- [16] Tianye Li, Timo Bolkart, Michael J Black, Hao Li, and Javier Romero. Learning a model of facial shape and expression from 4d scans. *ACM Trans. Graph.*, 36(6):194–1, 2017.
- [17] Xingchao Liu, Chengyue Gong, and Qiang Liu. Flow straight and fast: Learning to generate and transfer data with rectified flow. *arXiv preprint arXiv:2209.03003*, 2022.

[18] Yixin Liu, Kai Zhang, Yuan Li, Zhiling Yan, Chujie Gao, Ruoxi Chen, Zhengqing Yuan, Yue Huang, Hanchi Sun, Jianfeng Gao, et al. Sora: A review on background, technology, limitations, and opportunities of large vision models. *arXiv preprint arXiv:2402.17177*, 2024.

[19] William Peebles and Saining Xie. Scalable diffusion models with transformers. Dec 2022.

[20] Aram-Alexandre Pooladian, Heli Ben-Hamu, Carles Domingo-Enrich, Brandon Amos, Yaron Lipman, and Ricky TQ Chen. Multisample flow matching: Straightening flows with minibatch couplings. *arXiv preprint arXiv:2304.14772*, 2023.

[21] KR Prajwal, Rudrabha Mukhopadhyay, Vinay P Namboodiri, and CV Jawahar. Learning individual speaking styles for accurate lip to speech synthesis. In *Proceedings of the IEEE/CVF conference on computer vision and pattern recognition*, pages 13796–13805, 2020.

[22] KR Prajwal, Rudrabha Mukhopadhyay, Vinay P Namboodiri, and CV Jawahar. A lip sync expert is all you need for speech to lip generation in the wild. In *Proceedings of the 28th ACM international conference on multimedia*, pages 484–492, 2020.

[23] Andrey V. Savchenko. Hsemotion: High-speed emotion recognition library. *Software Impacts*, page 100433, Dec 2022.

[24] Steffen Schneider, Alexei Baevski, Ronan Collobert, and Michael Auli. wav2vec: Unsupervised pre-training for speech recognition. In *Interspeech 2019*, Sep 2019.

[25] Maximilian Seitzer. pytorch-fid: Fid score for pytorch, 2020.

[26] Sheng Shi, Xuyang Cao, Jun Zhao, and Guoxin Wang. Joyhallo: Digital human model for mandarin. *arXiv preprint arXiv:2409.13268*, 2024.

[27] Aliaksandr Siarohin, Stéphane Lathuilière, Sergey Tulyakov, Elisa Ricci, and Nicu Sebe. First order motion model for image animation. *Advances in neural information processing systems*, 32, 2019.

[28] Jascha Sohl-Dickstein, EricA. Weiss, Niru Maheswaranathan, and Surya Ganguli. Deep unsupervised learning using nonequilibrium thermodynamics. *arXiv: Learning, arXiv: Learning*, Mar 2015.

[29] Jiaming Song, Chenlin Meng, and Stefano Ermon. Denoising diffusion implicit models. *arXiv preprint arXiv:2010.02502*, 2020.

[30] Xusen Sun, Longhao Zhang, Hao Zhu, Peng Zhang, Bang Zhang, Xinya Ji, Kangneng Zhou, Daiheng Gao, Liefeng Bo, and Xun Cao. Vividtalk: One-shot audio-driven talking head generation based on 3d hybrid prior. *arXiv preprint arXiv:2312.01841*, 2023.

[31] Supasorn Suwajanakorn, Steven M Seitz, and Ira Kemelmacher-Shlizerman. Synthesizing obama: learning lip sync from audio. *ACM Transactions on Graphics (ToG)*, 36(4):1–13, 2017.

[32] Linrui Tian, Siqi Hu, Qi Wang, Bang Zhang, and Liefeng Bo. Emo2: End-effector guided audio-driven avatar video generation. *arXiv preprint arXiv:2501.10687*, 2025.

[33] Linrui Tian, Qi Wang, Bang Zhang, and Liefeng Bo. Emo: Emote portrait alive generating expressive portrait videos with audio2video diffusion model under weak conditions. In *European Conference on Computer Vision*, pages 244–260. Springer, 2024.

[34] Thomas Unterthiner, Sjoerd Van Steenkiste, Karol Kurach, Raphaël Marinier, Marcin Michalski, and Sylvain Gelly. Fvd: A new metric for video generation. 2019.

[35] Munender Varshney, Ravindra Yadav, Vinay P. Namboodiri, and Rajesh M Hegde. Learning speaker-specific lip-to-speech generation. In *2022 26th International Conference on Pattern Recognition (ICPR)*, pages 491–498, 2022.

[36] Kaisiyuan Wang, Qianyi Wu, Linsen Song, Zhuoqian Yang, Wayne Wu, Chen Qian, Ran He, Yu Qiao, and Chen Change Loy. Mead: A large-scale audio-visual dataset for emotional talking-face generation. In *European conference on computer vision*, pages 700–717. Springer, 2020.

[37] Ting-Chun Wang, Arun Mallya, and Ming-Yu Liu. One-shot free-view neural talking-head synthesis for video conferencing. In *2021 IEEE/CVF Conference on Computer Vision and Pattern Recognition (CVPR)*, Jun 2021.

[38] Mingwang Xu, Hui Li, Qingkun Su, Hanlin Shang, Liwei Zhang, Ce Liu, Jingdong Wang, Yao Yao, and Siyu Zhu. Hallo: Hierarchical audio-driven visual synthesis for portrait image animation. *arXiv preprint arXiv:2406.08801*, 2024.

[39] Sicheng Xu, Guojun Chen, Yu-Xiao Guo, Jiaolong Yang, Chong Li, Zhenyu Zang, Yizhong Zhang, Xin Tong, and Baining Guo. Vasa-1: Lifelike audio-driven talking faces generated in real time. *Advances in Neural Information Processing Systems*, 37:660–684, 2024.

[40] Zhuoyi Yang, Jiayan Teng, Wendi Zheng, Ming Ding, Shiyu Huang, Jiazheng Xu, Yuanming Yang, Wenyi Hong, Xiaohan Zhang, Guanyu Feng, et al. Cogvideox: Text-to-video diffusion models with an expert transformer. *arXiv preprint arXiv:2408.06072*, 2024.

[41] Zhenhui Ye, Ziyue Jiang, Yi Ren, Jinglin Liu, Jinzheng He, and Zhou Zhao. Geneface: Generalized and high-fidelity audio-driven 3d talking face synthesis. *arXiv preprint arXiv:2301.13430*, 2023.

[42] Zipeng Ye, Mengfei Xia, Ran Yi, Juyong Zhang, Yu-Kun Lai, Xuwei Huang, Guoxin Zhang, and Yong-jin Liu. Audio-driven talking face video generation with dynamic convolution kernels. *IEEE Transactions on Multimedia*, 25:2033–2046, 2022.

[43] Jianhui Yu, Hao Zhu, Liming Jiang, Chen Change Loy, Weidong Cai, and Wayne Wu. Celebv-text: A large-scale facial text-video dataset. In *Proceedings of the IEEE/CVF Conference on Computer Vision and Pattern Recognition*, pages 14805–14814, 2023.

[44] Egor Zakharov, Aleksei Ivakhnenko, Aliaksandra Shysheya, and Victor Lempitsky. Fast bi-layer neural synthesis of one-shot realistic head avatars. In *Computer Vision–ECCV 2020: 16th European Conference, Glasgow, UK, August 23–28, 2020, Proceedings, Part XII 16*, pages 524–540. Springer, 2020.

[45] Wenxuan Zhang, Xiaodong Cun, Xuan Wang, Yong Zhang, Xi Shen, Yu Guo, Ying Shan, and Fei Wang. Sadtalker: Learning realistic 3d motion coefficients for stylized audio-driven single image talking face animation. In *Proceedings of the IEEE/CVF conference on computer vision and pattern recognition*, pages 8652–8661, 2023.

[46] Zhimeng Zhang, Lincheng Li, Yu Ding, and Changjie Fan. Flow-guided one-shot talking face generation with a high-resolution audio-visual dataset. In *Proceedings of the IEEE/CVF conference on computer vision and pattern recognition*, pages 3661–3670, 2021.

[47] Hao Zhu, Wayne Wu, Wentao Zhu, Liming Jiang, Siwei Tang, Li Zhang, Ziwei Liu, and Chen Change Loy. Celebv-hq: A large-scale video facial attributes dataset. In *European conference on computer vision*, pages 650–667. Springer, 2022.